NOMENCLATURE

C_p = heat capacity at constant pressure, [B.t.u./(lb.$_m$)(° F.)]
D_p = psuedo particle diameter, ft.
G = mass flow rate, [lb.$_m$/(hr.)(ft.^{2})]
H = particle height, in.
k_E = effective thermal conductivity, [B.t.u./(hr.)(ft.)(° F.)]
N_{Re} = modified Reynolds number, dimensionless
R = particle radius, in.
r = packed bed radius, ft.
t = temperature, ° F.
z = packed bed depth from top to bottom, ft.
μ = viscosity, [lb.$_m$/(hr.)(ft.)]
ψ = (total particle suface/volume of particle), ft.$^{-1}$

ACKNOWLEDGMENT

The permission of the Phillips Petroleum Co. to publish this work is gratefully acknowledged.

LITERATURE CITED

(1) Kannuluick, W.G., Martin, L.H., *Proc. Royal Soc. (London)* A141, 144 (1933).
(2) Schumann, T.E.W., Voss, V., *Fuel* **13**, 249 (1934).
(3) Waddams, A.L., *Chem. Ind. (London)* **22**, 206 (1944).
(4) Weiniger, J.L., Schneider, W.G., *Ind. Eng. Chem.* **43**, 1229 (1951).
(5) Yagi, Sakae, Kunii, Daizo, A.I.Ch.E.J. **3**, 373 (1957).

RECEIVED for review June 27, 1963. Resubmitted November 18, 1963. Accepted February 20, 1964.

CHO Gas Phase Compositions in Equilibrium with Carbon, and Carbon Deposition Boundaries at One Atmosphere

E. J. CAIRNS and A. D. TEVEBAUGH
General Electric Research Laboratory, Schenectady, New York

Gas phase compositions in equilibrium with carbon (graphite) have been calculated for the full composition range of the CHO system and for temperatures in the range of 298° to 1500° K., all at atmospheric pressure. The equilibrium gas phase compositions are presented graphically as a function of the O/H atom ratio, and are discussed. The species of major importance were found to be C, CO, CO_2, H_2, H_2O, and CH_4. The species of secondary importance are C_2H_6, C_2H_4, and C_2H_2, while species such as CH_3OH, HCHO, C_2H_5OH, and $C_{10}H_{22}$ were found to be present in amounts several orders of magnitude below the amounts of the species of secondary importance. The amount of any trace component can be easily calculated from these data. The carbon deposition boundaries are presented on triangular coordinates and are discussed.

THE CHO SYSTEM is of great importance in many areas of modern technology, including fuel cells, combustion, gasification processes, hydrogen production, and chemical synthesis processes (*8, 9*). As a result, many studies, both experimental (*6, 12, 14, 15, 17, 18, 20, 23*) and theoretical (*2-4, 11, 19, 22*) have been carried out. However, the results on the thermodynamics of the CHO system available in the open literature are of rather limited scope, usually because of the small ranges of the variables covered in specific processes (*e.g.*, hydrocarbon or alcohol synthesis) of interest to those authors. All data available considered together cover but a small fraction of the total possible range of composition included in the CHO system.

This paper considers the CHO gas phase compositions in equilibrium with graphite over the temperature range 298–1500° K., at a pressure of one atmosphere, for O/H atomic ratios from 0.026 to 4.5, and the carbon deposition boundaries under the same conditions, except over the full range of O/H atomic ratios.

GENERAL THERMODYNAMIC CONSIDERATIONS

Before considering the computational methods, the system and chemical species of interest will be outlined, since they influence the choice of method. The species most likely to be present in the greatest amounts are among those which are most stable under the conditions of interest, *i.e.*, those having the lowest value of the free energy of formation. In the system containing the elements carbon, hydrogen, and oxygen, in the temperature range of 298° to 1500° K., and at a pressure of one atmosphere the most stable species are carbon, hydrogen, water, carbon dioxide, carbon monoxide, and methane, with other species such as ethane, methanol, and some of the other hydrocarbons being less stable. In order to perform a completely rigorous set of thermodynamic calculations, it would be necessary to consider every possible species containing the elements C, H, and O. The elimination of the very large number of high molecular weight species and their isomers from the equilibrium calculations on the basis of tabulated free energy of formation data alone is particularly difficult at low temperatures. These species would have very low vapor pressures and could collectively result in significant changes in the over-all gas phase composition. Fortunately, the inclusion of the high molecular weight species would not be realistic since it is observed that even at high temperatures, there are kinetic hindrances which reduce their rates of formation to insignificantly small values, allowing many syntheses of low molecular weight materials to take place, with only a very minute amount of tar formation. For these reasons, then, high molecular-weight materials will not be considered in this analysis. It must be resolved as to whether or not species in the C_2 to C_{10} range will be present in important amounts (*i.e.*, 1 mole in 10^6 moles of total products). First, a review of the equilibrium constants of formation for the species will give a rough approximation as to the relative importance of the various molecules. Consideration of equilibrium constant of formation data, which indicates the relative importance of the more stable species, shows that the most important species to consider are H_2O, CO_2, H_2, CO, C, and CH_4. The equilibrium constants of formation for H_2O and CO_2 are so large that the oxygen concentration will not be large enough to affect the sixth significant figure for the partial pressures of the various species reported here, even at 1500° K. Secondly, more quantitative evidence is given by considering the equations:

$$nC + (n+1)H_2 \longrightarrow C_nH_{2n+2} \qquad (1)$$

$$K_f = \frac{(p_{C_nH_{2n+2}})}{(p_{H_2})^{n+1}} \qquad (2)$$

$$(p_{C_nH_{2n+2}}) = K_f(p_{H_2})^{n+1} \qquad (3)$$

Low pressures favor the lower molecular weight species, and therefore in systems where the partial pressure of H_2 is much less than one atmosphere ($\sim 10^{-5}$ atm. at 298° K. as in the cases we are considering), the amount of gas phase paraffin species of higher molecular weight decreases with the (n + 1) power of the hydrogen partial pressure, where n is the number of carbon atoms in the species being considered.

On the basis of the above discussion, the six species H_2, H_2O, C, CH_4, CO, and CO_2 were deemed most important. A final check on the validity of this conclusion easily can be made after the calculations on the above six species are made. This check consists of calculating the partial pressure of the test species using Equation 3 or a similar equation together with the partial pressure of H_2 previously calculated and comparing the result to the partial pressures of the other components in the system. If this value is small compared to the other partial pressures, then it is valid to assume the absence of that species for the purposes of the calculations at hand.

METHODS FOR CALCULATION

The literature contains two general methods for calculating complex chemical equilibria applicable to the CHO system: Algebraic solutions of equilibrium constants and material balance equations (*1, 3-5, 6, 12, 14-20, 22*) and the minimization of the free energy of the system (*2, 10, 13, 19, 21, 22, 25*).

In this work, the direct algebraic solution of a set of nonlinear equations which were obtained from the material balance equations and the nonlinear form of the standard equilibrium constant equations was used.

Since the considerations of possible stable species of importance led to only six species of primary interest, it was possible to write fairly simple nonlinear algebraic equations, allowing solution in a few minutes on an IBM 650 computer, or in an hour on a desk calculator.

The system is composed of six components and two phases; the phase rule indicates that six constraints on the system are necessary for a complete definition of the system. These constraints were chosen to be temperature, pressure, one material balance constraint, and three equilibrium constant equations which collectively include all six species. As a material balance constraint, the condition of one mole total reactants (α moles of H_2O, β moles of CO_2 and $1-\alpha-\beta$ moles CH_4) containing a fixed O/H ratio was used. The gas phase composition, as readily shown by the phase rule, will be determined by the O/H ratio and will be independent of the chemical identity of the reactant gases. The three chemical equations chosen to link the six species through material balance and mass action laws were:

$$CH_4 \rightleftarrows C + 2H_2 \qquad K_1 \qquad (4)$$

$$C + H_2O(g) \rightleftarrows CO + H_2 \qquad K_2 \qquad (5)$$

$$CO + H_2O(g) \rightleftarrows CO_2 + H_2 \qquad K_3 \qquad (6)$$

A group of three species were chosen as the independent unknowns such that at least one appears in each of the above chemical equations. Upon application of the material balance constraint to the chemical equations, the equilibrium amounts of all six species can be written in terms of the chosen three. For the three independent unknowns CO_2, H_2O and H_2 were chosen, and expressed as x moles of CO_2, y moles of H_2O and z moles of H_2. The expressions for the equilibrium amounts of all six species in terms of x, y, and z are given in Table I.

Table I. Material Balance Expressions

Species	Moles at start	Moles at Equilibrium
C	0	$[\frac{1}{2}z + \frac{3}{2}y + x - \frac{3}{2}\alpha - \beta]$
CH_4	$1-\alpha-\beta$	$[1 - (\frac{1}{2}\alpha + \beta) - \frac{1}{2}(y+z)]$
CO	0	$[2(\beta - x) - (y - \alpha)]$
CO_2	β	x
H_2	0	z
H_2O	α	y
Total moles	1	$[1 - \alpha + y + z]$
Total gas moles	1	$[1 + \frac{1}{2}\alpha + \beta - x - \frac{1}{2}y + \frac{1}{2}z]$

The equation for x (moles of CO_2) in terms of y and z was obtained by substituting expressions from Table I into the equilibrium constant equation for Reaction (*6*), and solving for x.

$$x = \frac{K_3[\alpha + 2\beta - y]y}{(z + 2K_3y)} \qquad (7)$$

Similar equilibrium constant equations for Reactions 4 and 5 were written and an equation for y in terms of z was derived after eliminating x between the two equilibrium constant equations:

$$y = \frac{K_1(2+z)(1 - \frac{1}{2}z - \frac{1}{2}\alpha - \beta) - 2z^2}{\frac{1}{2}K_1(2+z) - K_2z} \qquad (8)$$

By progressive elimination of unknowns, a simple polynominal in z (moles of H_2) was obtained:

$$C_5z^5 + C_4z^4 + C_3z^3 + C_2z^2 + C_1z + C_0 = 0 \qquad (9)$$

The solution of Equation 9 for z, Equation 8 for y and Equation 7 for x requires about an hour using a desk calculator.

where

$$C_0 = 8K_1^2K_2K_3\,(1 - \tfrac{1}{2}\alpha - \beta)^2$$

$$C_1 = K_1^2K_2(\tfrac{1}{2}\alpha + \beta - 1)\,[12K_3(\tfrac{1}{2}\alpha + \beta - \tfrac{1}{3}) - 4(\tfrac{1}{2}\alpha + \beta)]$$

$$C_2 = K_1\langle[2(1 - \tfrac{1}{2}\alpha - \beta)\{K_1(\tfrac{1}{2}K_2 + 1) - 2K_2[K_1(\tfrac{1}{2}\alpha + \beta)(K_3 - \tfrac{1}{2}) + 2K_3(\tfrac{1}{2}K_1 + 2)]\} + K_2(1 + \tfrac{1}{2}\alpha + \beta)[K_1(1-\alpha-2\beta) + 2K_2(\tfrac{1}{2}\alpha + \beta - 1)] + K_1(\alpha + 2\beta)[K_2K_3(\tfrac{1}{2}\alpha + \beta) - 1]\rangle$$

$$C_3 = K_1\{K_2(K_3 - \tfrac{1}{2})[(\tfrac{1}{2}\alpha + \beta)^2K_1 - 4(1 - \tfrac{1}{2}\alpha - \beta)(\tfrac{1}{2}K_1 + 2)] + K_2(\tfrac{1}{2}K_1 + 2)[4(\tfrac{1}{2}\alpha + \beta)K_3 - (1 + \tfrac{1}{2}\alpha + \beta)] + (\tfrac{1}{2}\alpha + \beta)(K_2 - \tfrac{1}{2}K_1)[4 + K_2(1 + \tfrac{1}{2}\alpha + \beta)] + (\tfrac{1}{2}K_2 + 1)[K_1(1-\alpha-2\beta) + 2K_2(\tfrac{1}{2}\alpha + \beta - 1)]\}$$

$$C_4 = 2K_2(\tfrac{1}{2}K_1 + 2)[K_1(K_3 - \tfrac{1}{2})(\tfrac{1}{2}\alpha + \beta) + K_3(\tfrac{1}{2}K_1 + 2)] + (K_2 - \tfrac{1}{2}K_1)[2(\tfrac{1}{2}\alpha + \beta)(\tfrac{1}{2}K_1 - K_2) + K_2(1 + \tfrac{1}{2}\alpha + \beta)(\tfrac{1}{2}K_1 + 2)] - K_1(\tfrac{1}{2}K_2 + 1)[(\tfrac{1}{2}\alpha + \beta)(\tfrac{1}{2}K_1 - K_2) + (\tfrac{1}{2}K_1 + 2)]$$

$$C_5 = (\tfrac{1}{2}K_1 + 2)[K_2(K_3 - \tfrac{1}{2})(\tfrac{1}{2}K_1 + 2) - (\tfrac{1}{2}K_2 + 1)(\tfrac{1}{2}K_1 - K_2)]$$

Table II. Gas Phase Compositions in Equilibrium with Solid Carbon

		Product Partial Pressures (Atm.)				
O/H	T, ° K.	H_2	CO	CH_4	$H_2O(g)$	CO_2
0.0263158	[a] 298	3.37198×10^{-5}	2.96524×10^{-13}	9.00055×10^{-1}	9.98240×10^{-2}	8.71385×10^{-5}
	500	1.81753×10^{-2}	1.24855×10^{-6}	8.83613×10^{-1}	9.73313×10^{-2}	8.79336×10^{-4}
	700	2.68525×10^{-1}	7.32615×10^{-4}	6.46949×10^{-1}	8.17822×10^{-2}	2.01117×10^{-3}
	900	7.55471×10^{-1}	2.04476×10^{-2}	1.85497×10^{-1}	3.64132×10^{-2}	2.17162×10^{-3}
	1100	9.17487×10^{-1}	4.75839×10^{-2}	3.09528×10^{-2}	3.79118×10^{-3}	1.85749×10^{-4}
	1300	9.42590×10^{-1}	4.99349×10^{-2}	7.04809×10^{-3}	4.14963×10^{-4}	1.19479×10^{-5}
	1500	9.47587×10^{-1}	5.00368×10^{-2}	2.29584×10^{-3}	7.89073×10^{-5}	1.54343×10^{-6}
0.0405405	[a] 298	3.27721×10^{-5}	4.57005×10^{-13}	8.50177×10^{-1}	1.49583×10^{-1}	2.07062×10^{-4}
	500	1.76757×10^{-2}	1.90303×10^{-6}	8.53701×10^{-1}	1.44570×10^{-1}	2.05120×10^{-3}
	700	2.61363×10^{-1}	1.10498×10^{-3}	6.12897×10^{-1}	1.20060×10^{-1}	4.57517×10^{-3}
	900	7.36139×10^{-1}	3.03298×10^{-2}	1.76124×10^{-1}	5.26292×10^{-2}	4.77790×10^{-3}
	1100	8.93419×10^{-1}	7.12833×10^{-2}	2.93502×10^{-2}	5.53029×10^{-3}	4.16850×10^{-4}
	1300	9.17796×10^{-1}	7.48885×10^{-2}	6.68223×10^{-3}	6.06375×10^{-4}	2.68912×10^{-5}
	1500	9.22655×10^{-1}	7.50499×10^{-2}	2.17658×10^{-3}	1.15324×10^{-4}	3.47481×10^{-6}
0.0555556	[a] 298	3.17975×10^{-5}	6.27422×10^{-13}	8.00362×10^{-1}	1.99216×10^{-1}	3.90204×10^{-4}
	500	1.71674×10^{-2}	$2.588 \quad \times 10^{-6}$	7.88332×10^{-1}	1.90712×10^{-1}	3.78398×10^{-3}
	700	2.54168×10^{-1}	1.48124×10^{-3}	5.79618×10^{-1}	1.56511×10^{-1}	8.22147×10^{-3}
	900	7.16954×10^{-1}	4.00231×10^{-2}	1.67064×10^{-1}	6.76394×10^{-2}	8.31992×10^{-3}
	1100	8.69378×10^{-1}	9.49252×10^{-2}	2.77918×10^{-2}	7.16617×10^{-3}	7.39196×10^{-4}
	1300	8.93006×10^{-1}	9.98328×10^{-2}	6.32583×10^{-3}	7.87620×10^{-4}	4.78559×10^{-5}
	1500	8.97724×10^{-1}	1.00060×10^{-1}	$2.0607 \quad \times 10^{-3}$	1.49404×10^{-4}	6.16849×10^{-6}
0.0882353	[a] 298	2.97578×10^{-5}	9.99985×10^{-9}	7.00972×10^{-1}	2.98001×10^{-1}	9.97120×10^{-4}
	500	1.61248×10^{-2}	$4.037 \quad \times 10^{-6}$	6.95487×10^{-1}	2.79192×10^{-1}	9.19224×10^{-3}
	700	2.39694×10^{-1}	2.24492×10^{-3}	5.15481×10^{-1}	2.23696×10^{-1}	1.88843×10^{-2}
	900	6.78911×10^{-1}	5.89329×10^{-2}	1.49805×10^{-1}	9.43124×10^{-2}	1.80391×10^{-2}
	1100	8.21360×10^{-1}	1.42047×10^{-1}	2.48066×10^{-2}	1.01313×10^{-2}	1.65525×10^{-3}
	1300	8.43435×10^{-1}	1.49699×10^{-1}	5.64298×10^{-3}	1.11566×10^{-3}	1.07621×10^{-4}
	1500	8.47866×10^{-1}	1.50070×10^{-1}	$1.8379 \quad \times 10^{-3}$	2.11968×10^{-4}	1.38975×10^{-5}
0.125000	[a] 298	2.75777×10^{-5}	1.43788×10^{-12}	6.02027×10^{-1}	3.95896×10^{-1}	2.04902×10^{-3}
	500	1.50476×10^{-2}	$5.5876 \quad \times 10^{-6}$	6.05667×10^{-1}	3.61576×10^{-1}	1.77038×10^{-2}
	700	2.25128×10^{-1}	3.02255×10^{-3}	4.54735×10^{-1}	2.82881×10^{-1}	3.42332×10^{-2}
	900	6.41148×10^{-1}	7.73263×10^{-2}	1.33603×10^{-1}	1.16865×10^{-1}	3.10567×10^{-2}
	1100	7.73412×10^{-1}	1.88973×10^{-1}	2.19949×10^{-2}	1.26915×10^{-2}	2.92954×10^{-3}
	1300	7.93874×10^{-1}	1.99537×10^{-1}	4.99953×10^{-3}	1.39906×10^{-3}	1.91121×10^{-4}
	1500	7.98013×10^{-1}	2.00069×10^{-1}	1.62827×10^{-3}	2.65777×10^{-4}	2.46824×10^{-5}
0.214286	[a] 298	2.26651×10^{-5}	2.59259×10^{-12}	4.06646×10^{-1}	5.86670×10^{-1}	6.66148×10^{-3}
	500	1.27991×10^{-2}	9.13115×10^{-6}	4.38186×10^{-1}	5.01863×10^{-1}	4.71425×10^{-2}
	700	1.95833×10^{-1}	4.61447×10^{-3}	3.44091×10^{-1}	3.75672×10^{-1}	7.97895×10^{-2}
	900	5.65895×10^{-1}	1.12991×10^{-1}	1.04081×10^{-1}	1.50722×10^{-1}	6.63107×10^{-2}
	1100	6.77643×10^{-1}	2.82321×10^{-1}	1.68850×10^{-2}	1.66128×10^{-2}	6.53860×10^{-3}
	1300	6.94772×10^{-1}	2.99133×10^{-1}	3.82905×10^{-3}	1.83648×10^{-3}	4.29742×10^{-4}
	1500	6.98313×10^{-1}	3.00036×10^{-1}	$1.2470 \quad \times 10^{-3}$	3.48528×10^{-4}	5.54704×10^{-5}

(*Continued on page 456*)

Application of the material balance constraint to the equilibrium constant equations provides for the expression of whether carbon is deposited from the reactant mixture, or is consumed and to what extent, during the establishment of equilibrium. A negative carbon result indicates consumption of carbon by the reactant gases in the amount indicated by the negative value; a positive carbon result means that carbon was deposited in the amount calculated.

It is clear from the above discussion that all of the present calculations apply to the case where solid carbon is in equilibrium with the gas phase. For the situation where solid carbin is absent, somewhat different equations must be used.

Since a large number of results were desired from these equations, a simple program was written for the IBM 650 digital computer. A complete solution of this program for one temperature and initial gas composition was obtained in about two minutes. The input data for the computer were tabulated values of temperature, α, β, and $\log_{10}$ of K_1, K_2, and K_3. The source of the equilibrium data was APIRP # 44 (*24*).

RESULTS AND DISCUSSION

The gas phase compositions in equilibrium with solid carbon for various O/H ratios are shown in Table II. The ranges covered by the table are O/H ratios of 0.026 to 4.5 and temperatures of 298° to 1500° K. This method of tabulation is especially useful in connection with processes of progressive oxidation, and in cases where either the hydrogen or oxygen content is varied. The system is determined by the O/H ratio for a given temperature and pressure. Table III contains the data for the trace species. The data are summarized in Figures 1 through 6.

All of the values presented for 298° K. were calculated as if all the water present existed in the gas phase. In fact, this is only true for H_2O partial pressures less than the vapor pressure of pure H_2O. The 298° K. values in Table II are useful for interpolation purposes and do not reflect the true equilibrium that would exist in the presence of liquid H_2O.

Accuracy of Results and Influence of Trace Constituents. The limiting accuracy of the calculated data (which were calculated to six figures) is that of the equilibrium constants used (*24*). The reported accuracy (*24*) of the equilibrium constants varies with temperature in the following manner: at 900° K., the values are reported to be accurate to four significant figures, while at the temperature extremes five figures are reported to be significant. This limiting accuracy will apply to the present results when the equilibrium mixture contains but minute amounts of species other than those included in the equilibrium calculations. In order

Table II. Gas Phase Composition in Equilibrium with Solid Carbon (*Continued*)

		Product Partial Pressures (Atm.)				
O/H	T, ° K.	H_2	CO	CH_4	$H_2O(g)$	CO_2
0.333333	[a] 298	1.66915×10^{-5}	4.55388×10^{-12}	2.20542×10^{-1}	7.58889×10^{-1}	2.05524×10^{-2}
	500	1.04711×10^{-2}	1.3270×10^{-5}	2.93283×10^{-1}	5.96673×10^{-1}	9.95602×10^{-2}
	700	1.66509×10^{-1}	6.24557×10^{-3}	2.48757×10^{-1}	4.32324×10^{-1}	1.46165×10^{-1}
	900	4.90301×10^{-1}	1.47661×10^{-1}	7.81315×10^{-2}	1.70658×10^{-1}	1.13248×10^{-1}
	1100	5.81912×10^{-1}	3.75136×10^{-1}	1.24513×10^{-2}	1.89560×10^{-2}	1.15446×10^{-2}
	1300	5.95678×10^{-1}	3.98646×10^{-1}	2.81469×10^{-3}	2.09829×10^{-3}	7.63205×10^{-4}
	1500	5.98617×10^{-1}	3.99969×10^{-1}	9.159×10^{-4}	3.99053×10^{-4}	9.87661×10^{-5}
0.409091	[a] 298	1.32268×10^{-5}	6.23230×10^{-12}	1.38487×10^{-1}	8.23005×10^{-1}	3.84943×10^{-2}
	500	9.30875×10^{-3}	1.5547×10^{-5}	2.31784×10^{-1}	6.21996×10^{-1}	1.36896×10^{-1}
	700	1.51905×10^{-1}	7.07189×10^{-3}	2.07035×10^{-1}	4.46588×10^{-1}	1.87400×10^{-1}
	900	4.52169×10^{-1}	1.64764×10^{-1}	6.64513×10^{-2}	1.75615×10^{-1}	1.41001×10^{-1}
	1100	5.34014×10^{-1}	4.21392×10^{-1}	1.04859×10^{-2}	1.95407×10^{-2}	1.45671×10^{-2}
	1300	5.46127×10^{-1}	4.48378×10^{-1}	2.36583×10^{-3}	2.16403×10^{-3}	9.65636×10^{-4}
	1500	5.48769×10^{-1}	4.49922×10^{-1}	7.67854×10^{-4}	4.14902×10^{-4}	1.26006×10^{-4}
0.750000	[a] 298	5.09532×10^{-6}	1.49179×10^{-11}	2.05515×10^{-2}	7.58890×10^{-1}	2.20554×10^{-1}
	500	6.03463×10^{-3}	2.2990×10^{-5}	9.74095×10^{-2}	5.96723×10^{-1}	2.99809×10^{-1}
	700	1.08621×10^{-1}	9.57532×10^{-3}	1.05859×10^{-1}	4.32382×10^{-1}	3.43563×10^{-1}
	900	3.35650×10^{-1}	2.15629×10^{-1}	3.66162×10^{-2}	1.70606×10^{-1}	2.41499×10^{-1}
	1100	3.89962×10^{-1}	5.59784×10^{-1}	5.59171×10^{-3}	1.89558×10^{-2}	2.57064×10^{-2}
	1300	3.97422×10^{-1}	5.97518×10^{-1}	1.25287×10^{-3}	2.09845×10^{-3}	1.71472×10^{-3}
	1500	3.99198×10^{-1}	5.99775×10^{-1}	4.077×10^{-4}	3.98019×10^{-4}	2.21515×10^{-4}
1.03846	[a] 298	3.32937×10^{-6}	1.90266×10^{-11}	8.77459×10^{-3}	6.32446×10^{-1}	3.58776×10^{-1}
	500	4.60012×10^{-3}	2.6848×10^{-5}	5.66028×10^{-2}	5.30691×10^{-1}	4.08080×10^{-1}
	700	8.74048×10^{-2}	1.08317×10^{-2}	6.85441×10^{-2}	3.93580×10^{-1}	4.39639×10^{-1}
	900	2.75847×10^{-1}	2.41011×10^{-1}	2.47307×10^{-2}	1.56713×10^{-1}	3.01699×10^{-1}
	1100	3.17623×10^{-1}	6.28879×10^{-1}	3.70958×10^{-3}	1.73452×10^{-2}	3.24440×10^{-2}
	1300	3.23024×10^{-1}	6.72061×10^{-1}	8.27749×10^{-4}	1.91834×10^{-3}	2.16921×10^{-3}
	1500	3.24395×10^{-1}	6.74691×10^{-1}	2.6910×10^{-4}	3.64299×10^{-4}	2.80666×10^{-4}
2.00000	[a] 298	1.60886×10^{-6}	2.4647×10^{-11}	2.04899×10^{-3}	3.95900×10^{-1}	6.02049×10^{-1}
	500	2.55093×10^{-3}	3.2987×10^{-5}	1.74059×10^{-2}	3.62121×10^{-1}	6.17890×10^{-1}
	700	5.28567×10^{-2}	1.29181×10^{-2}	2.50669×10^{-2}	2.83855×10^{-1}	6.25304×10^{-1}
	900	1.73290×10^{-1}	2.83544×10^{-1}	9.75998×10^{-3}	1.15823×10^{-1}	4.17582×10^{-1}
	1100	1.96380×10^{-1}	7.44092×10^{-1}	1.41807×10^{-3}	1.26889×10^{-2}	4.54206×10^{-2}
	1300	1.98924×10^{-1}	7.96316×10^{-1}	3.13887×10^{-4}	1.39980×10^{-3}	3.04556×10^{-3}
	1500	1.99683×10^{-1}	7.99555×10^{-1}	1.020×10^{-4}	2.65731×10^{-4}	3.94140×10^{-4}
4.50000	[a] 298	7.02149×10^{-7}	2.84185×10^{-11}	3.90300×10^{-4}	1.99219×10^{-1}	8.00390×10^{-1}
	500	1.18110×10^{-3}	3.7787×10^{-5}	3.73142×10^{-3}	1.91234×10^{-1}	8.03816×10^{-1}
	700	2.60394×10^{-2}	1.45710×10^{-2}	6.08361×10^{-3}	1.57732×10^{-1}	7.95574×10^{-1}
	900	8.82078×10^{-2}	3.17980×10^{-1}	2.52882×10^{-3}	6.61159×10^{-2}	5.25168×10^{-1}
	1100	9.86138×10^{-2}	8.36468×10^{-1}	3.57600×10^{-4}	7.16286×10^{-3}	5.73981×10^{-2}
	1300	9.95270×10^{-2}	8.95753×10^{-1}	7.85691×10^{-5}	7.87818×10^{-4}	3.85365×10^{-3}
	1500	9.98669×10^{-2}	8.99459×10^{-1}	2.5517×10^{-5}	1.49518×10^{-4}	4.98830×10^{-4}

[a] These are the values that would hold if all of the water present could exist in the gas phase.

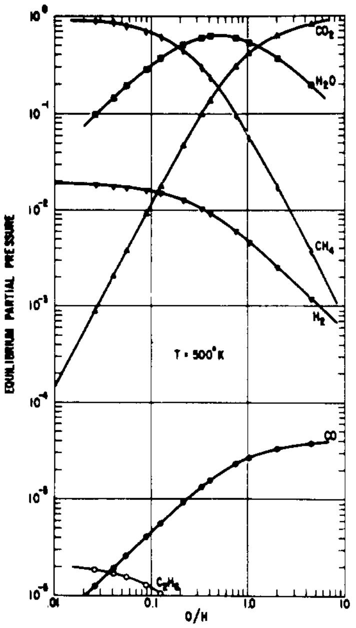

Figure 1. Equilibrium partial pressures in the CHO system as a function of O/H atom ratio at 1 atmosphere and 500° K.

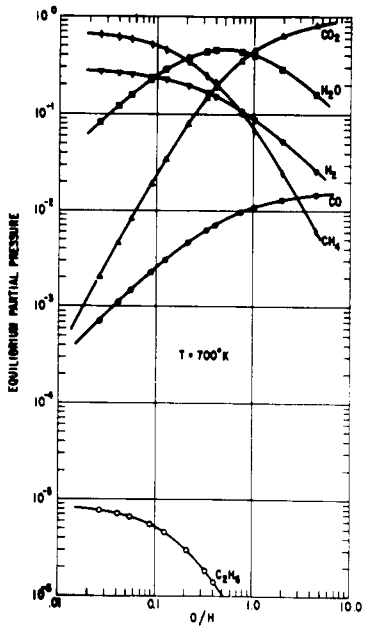

Figure 2. Equilibrium partial pressures in the CHO system as a function of O/H atom ratio at 1 atmosphere and 700° K.

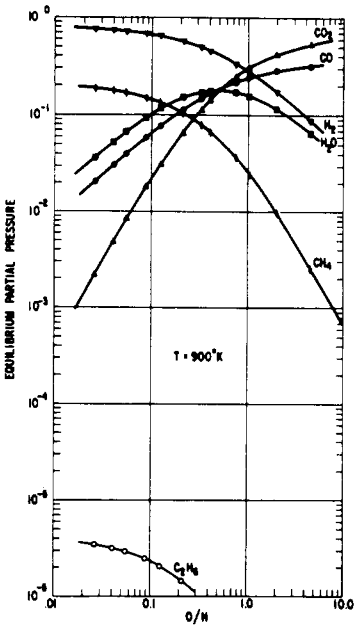

Figure 3. Equilibrium partial pressures in the CHO system as a function of O/H atom ratio at 1 atmosphere and 900° K.

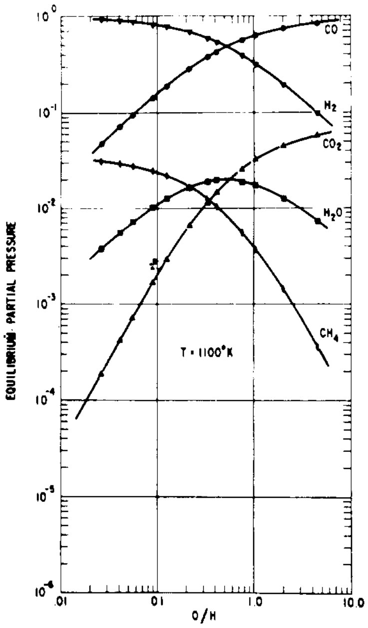

Figure 4. Equilibrium partial pressures in the CHO system as a function of O/H atom ratio at 1 atmosphere and 1100° K.

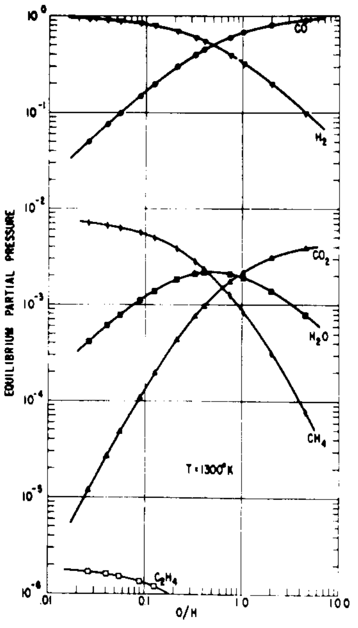

Figure 5. Equilibrium partial pressures in the CHO system as a function of O/H atom ratio at 1 atmosphere and 1300° K.

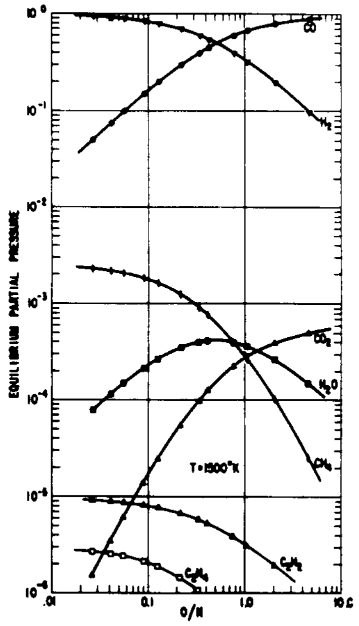

Figure 6. Equilibrium partial pressures in the CHO system as a function of O/H atom ratio at 1 atmosphere and 1500° K.

to evaluate the magnitude of the error resulting from limiting the calculations to the system containing only CH_4, H_2, C, CO, CO_2, and H_2O, the equilibrium amounts of the other species most likely to be present (CH_3OH, C_2H_6, C_2H_4, C_2H_2, C_2H_5OH, $C_{10}H_{22}$, and HCHO) were calculated from equations similar to (3) and partial pressure data from Figures 1–6. It was found that C_2H_5OH, $C_{10}H_{22}$, and HCHO were present in amounts several orders of magnitude below the values found for CH_3OH, C_2H_6, C_2H_4, and C_2H_2. The partial pressures of all these species were less than 2×10^{-5} atmospheres for all the conditions considered here. At 1400° K. and above, trace amounts of species such as atomic hydrogen and methyl radicals are present in amounts similar to that of C_2H_2 (*11*). Therefore, extrapolation of these results to temperatures above 1500° K. should be approached with caution. It is valid to calculate the amounts of any of these other species in the manner indicated above if they are present in amounts too low to significantly alter the equilibrium compositions reported from the original calculations. The calculated partial pressures of the trace species are shown in Figures 1–6, where the amounts were great enough to be plotted. The influence of these trace species on the values shown in Figures 1–6 for the major species was determined by assuming the extreme case of all of the hydrogen required to form the trace species being supplied from the hydrogen gas in Figures 1–6. The amount required (as calculated from the equilibrium constant of formation for the trace species) was then deducted from the hydrogen value in Figures 1–6. The influence of this change in the hydrogen value on the other equilibrium constants for the system was such that the values of Figures 1–6 were found to be unaffected to 5 significant figures, even when 2×10^{-5} moles of C_2H_2 were present at 1500° K.; and unaffected to 6 significant figures when 1×10^{-5} moles of C_2H_6 were present at 700° K. The results (to six figures) are not influenced at lower temperatures.

Since the presence of minor species does not appreciably alter the results, it is possible to use the reported gas phase compositions to calculate the amount of any minor gas phase constituent.

On the basis of the above discussion one can conclude that the present results are as accurate as the log K values (*24*).

Relationship to Phase Rule. Of the 18 reactant mixture compositions studied, six pairs were chosen to have identical O/H atom ratios, while having different reactant gas compositions. The results showed that the gas-phase compositions were identical for the pairs of cases with identical O/H atom ratios. The correspondence in gas-phase composition for identical O/H ratios follows from phase rule prediction:

$$F = C - P + 2$$

Components: C, H, O (3)
Phases: gas, solid (2) ·
∴ Degrees of freedon = 3; temperature, pressure (1 atm), and O/H ratio.

For such systems in equilibrium with solid carbon (graphite), the gas phase composition is completely determined by the temperature, pressure and O/H ratio.

General Trends. At all temperatures studied, the CH_4 partial pressure decreases smoothly by about two orders of magnitude due to oxidation as the O/H ratio increases from 0.02 to 4.5. The general level of CH_4 partial pressure decreases with increasing temperature due to thermal instability. As a special case, the CH_4 partial pressure at high O/H values shows a maximum near 700° K. probably due to competition between the following two reactions:

$$CH_4 \rightleftarrows C + 2H_2 \tag{10}$$

$$CO + 3H_2 \rightleftarrows CH_4 + H_2O \tag{11}$$

Reaction 10 is favored at high temperatures, while Reaction 11 is favored near 700° K. because of the rapid increase in the partial pressures of both CO and H_2, most evident at high O/H ratios.

Over the entire temperature range the H_2 partial pressure decreases smoothly due to oxidation through about one order of magnitude as the O/H ratio increases from 0.02 to. 4.5. The general level of the H_2 partial pressure increases with increasing temperature due to the decomposition of CH_4, and the gasification of carbon.

At all temperatures, the partial pressure of CO_2 increases by two to three orders of magnitude as the O/H ratio increases similarly, because CO_2 is an oxidation product of both CH_4 and solid carbon. The concentration of CO_2 is insensitive to temperature below 900° K. Above this value, CO_2 decreases rapidly with temperature due to the Boudouard equilibrium ($CO_2 + C \rightleftarrows 2CO$).

The CO partial pressure is more sensitive to temperature than to the O/H ratio below 900° K. Above 900° K., the CO partial pressure has reached almost one atmosphere and is insensitive to temperature because of the shift in the Boudouard equilibrium toward CO, and because of the excess of solid carbon (graphite) available. In addition, CO is also favored by the equilibrium ($H_2O + C \rightleftarrows CO + H_2$), while the amount of H in the system is fixed.

The partial pressure of H_2O increases with the O/H ratio (since it is an oxidation product), until a maximum value is achieved at the stoichiometric point (O/H = 0.5), whereupon the partial pressure decreases with further increases in the O/H ratio, primarily due to the dilution effects of the CO and CO_2 produced from the excess of solid carbon present. For a given O/H ratio, the H_2O partial pressure decreases with increasing temperature, mainly due to its consumption in the carbon gasification reactions.

Generally, CH_4 is the most important species at low temperatures and low O/H ratios. As oxidation proceeds at low temperatures, H_2O and CO_2 are the major oxidation products. Near 900° K., all gaseous species are present in nearly the same amounts over the O/H range of 0.1 to 1.0. This behavior is expected in view of the fact that the equilibrium constants of these species are all nearly one at 900° K. At 1100° K. and above, H_2 and CO are the most important species. At 1500K K., no other species are present in excess of 3×10^{-3} atmospheres partial pressure. Since CO is the most stable oxidation product at high temperatures, H_2 and CO are the primary species present and will exist in equal amounts when O/H = 0.5 (*i.e.*, $O/H_2 = CO/H_2 = 1$).

The main reason for the decreasing partial pressures of H_2 and H_2O at O/H ratios >0.5 is the dilution effect due to the formation of CO and/or CO_2 from the solid carbon phase.

By far, the most rapid changes in the partial pressures of all species occurs in the range 0 to 0.5 O/H at all temperatures. This effect is most evident when the data are plotted on a linear O/H scale. In the O/H range below 0.5, the gaseous species are being oxidized, while above this value, the main oxidation is that of solid carbon, adding to the gas phase.

Relationships Among Species. Relatively simple relationships among the species exist because the gas phase is in equilibrium with solid carbon, fixing its chemical potential at a constant value for a given temperature. Equation 12 shows that the CH_4 partial pressure varies:

$$CH_4 \rightleftarrows 2H_2 + C \ldots\ldots\ldots K_6 \tag{12}$$

$$[CH_4] = \frac{[H_2]^2}{K_6}$$

as the square of the H_2 partial pressure. Equation 13 shows that the CO_2 partial pressure varies with the square of the CO

$$2CO \rightleftarrows CO_2 + C \ldots\ldots\ldots K_7 \tag{13}$$

$$[CO_2] = K_7[CO]^2$$

partial pressure, and Equation 14 show that the H_2O partial pressure varies directly as the product of the H_2 and CO partial pressures.

$$CO + H_2 \rightleftarrows H_2O + C \ldots\ldots\ldots K_8 \tag{14}$$

$$[H_2O] = K_8[CO][H_2]$$

Table III. Equilibrium Compositions of Minor Constituents in Contact with Solid Carbon and at a Total Pressure of one Atmosphere

		Product Partial Pressures (Atm.)			
O/H	T, ° K.	CH_3OH	C_2H_6	C_2H_4	C_2H_2
0.0263158	298	...	2.21×10^{-8}	...	...
	500	2.51×10^{-12}	1.85×10^{-6}	1.28×10^{-12}	4.27×10^{-23}
	700	...	7.68×10^{-6}	...	...
	900	6.36×10^{-10}	3.42×10^{-6}	2.27×10^{-7}	5.11×10^{-11}
	1100	1.58×10^{-10}	4.71×10^{-7}	8.58×10^{-7}	...
	1300	...	...	1.69×10^{-6}	6.01×10^{-7}
	1500	8.09×10^{-12}	2.27×10^{-8}	2.68×10^{-6}	9.19×10^{-6}
0.0405405	298	...	2.03×10^{-8}	...	...
	500	3.62×10^{-12}	1.70×10^{-6}	1.21×10^{-12}	4.15×10^{-23}
	700	...	7.08×10^{-6}	...	...
	900	8.96×10^{-10}	3.17×10^{-6}	2.16×10^{-7}	4.98×10^{-11}
	1100	2.25×10^{-10}	4.35×10^{-7}	8.13×10^{-7}	...
	1300	...	...	1.60×10^{-6}	5.85×10^{-7}
	1500	1.15×10^{-11}	2.09×10^{-8}	2.54×10^{-6}	8.95×10^{-6}
0.0555556	298	...	1.86×10^{-8}	...	...
	500	4.64×10^{-12}	1.56×10^{-6}	...	...
	700	...	6.51×10^{-6}	...	...
	900	1.12×10^{-9}	2.92×10^{-6}	...	...
	1100	2.83×10^{-10}	4.01×10^{-7}	7.70×10^{-7}	...
	1300	...	...	1.52×10^{-6}	5.69×10^{-7}
	1500	1.45×10^{-11}	...	2.41×10^{-6}	8.70×10^{-6}
0.0882353	298	...	...	...	...
	500	...	1.29×10^{-6}	1.01×10^{-12}	...
	700	...	5.46×10^{-6}	...	...
	900	...	2.48×10^{-6}	1.84×10^{-7}	...
	1100	...	3.38×10^{-7}	6.87×10^{-7}	...
	1300	...	...	1.35×10^{-6}	5.38×10^{-7}
	1500	...	...	2.15×10^{-6}	8.22×10^{-6}
0.125000	298	...	...	...	...
	500	...	1.05×10^{-6}	8.77×10^{-13}	...
	700	...	4.52×10^{-6}	...	...
	900	...	2.09×10^{-6}	1.64×10^{-7}	...
	1100	...	2.82×10^{-7}	6.10×10^{-7}	...
	1300	...	...	1.20×10^{-6}	5.06×10^{-7}
	1500	...	...	1.90×10^{-6}	7.74×10^{-6}
0.214286	298	...	...	...	...
	500	...	6.47×10^{-7}	6.35×10^{-13}	...
	700	...	2.98×10^{-6}	...	...
	900	...	1.44×10^{-6}	1.28×10^{-7}	...
	1100	...	1.90×10^{-7}	4.68×10^{-7}	...
	1300	...	...	9.19×10^{-7}	4.43×10^{-7}
	1500	...	...	1.46×10^{-6}	6.77×10^{-6}
0.333333	298	...	...	...	...
	500	...	3.54×10^{-7}	4.25×10^{-13}	...
	700	...	1.83×10^{-6}	...	...
	900	...	9.35×10^{-7}	9.58×10^{-8}	...
	1100	...	1.20×10^{-7}	3.45×10^{-7}	...
	1300	...	...	6.75×10^{-7}	3.80×10^{-7}
	1500	...	...	1.07×10^{-6}	5.81×10^{-6}
0.409091	298	...	...	...	...
	500	8.22×10^{-12}	2.49×10^{-7}	3.36×10^{-13}	2.19×10^{-23}
	700	...	1.39×10^{-6}	...	...
	900	...	7.33×10^{-7}	8.14×10^{-8}	3.06×10^{-11}
	1100	4.75×10^{-10}	...	...	8.17×10^{-9}
	1300	...	...	...	3.48×10^{-7}
	1500	2.44×10^{-11}	4.40×10^{-9}	8.99×10^{-7}	5.32×10^{-6}
0.750000	298	...	...	...	...
	500	...	6.78×10^{-8}	1.41×10^{-13}	...
	700	...	5.08×10^{-7}	...	...
	900	...	3.00×10^{-7}	4.49×10^{-8}	...
	1100	...	3.62×10^{-8}	1.55×10^{-7}	...
	1300	...	...	3.01×10^{-7}	2.53×10^{-7}
	1500	...	...	4.76×10^{-7}	3.87×10^{-6}
1.03846	298	...	...	...	...
	500	...	3.00×10^{-8}	8.20×10^{-14}	...
	700	...	2.65×10^{-7}	...	...
	900	...	1.67×10^{-7}	3.03×10^{-8}	...
	1100	...	1.95×10^{-8}	1.03×10^{-7}	...
	1300	...	...	1.99×10^{-7}	2.06×10^{-7}
	1500	...	...	3.14×10^{-7}	3.15×10^{-6}
	298	...	...	...	...
	500	...	5.12×10^{-9}	2.52×10^{-14}	...
	700	...	5.85×10^{-8}	...	...

(Continued on page 460)

Table III. Equilibrium Compositions of Minor Constituents in Contact with Solid Carbon and at a Total Pressure of one Atmosphere (*Continued*)

		Product Partial Pressures (Atm.)			
O/H	T, ° K.	CH_3OH	C_2H_6	C_2H_4	C_2H_2
2.00000	900	. . .	4.13×10^{-8}	1.20×10^{-6}	. . .
	1100	. . .	4.62×10^{-9}	3.93×10^{-8}	. . .
	1300	. . .	. . .	7.53×10^{-8}	1.27×10^{-7}
	1500	. . .	. . .	1.19×10^{-7}	1.94×10^{-6}
	298	. . .	. . .	. . .	. . .
	500	3.21×10^{-13}	5.09×10^{-10}	5.40×10^{-15}	2.78×10^{-24}
	700	. . .	. . .	. . .	. . .
4.50000	900	1.35×10^{-10}	5.44×10^{-9}	3.10×10^{-9}	5.96×10^{-12}
	1100	3.21×10^{-11}	. . .	. . .	1.51×10^{-9}
	1300	. . .	. . .	. . .	. . .
	1500	1.61×10^{-12}	2.65×10^{-11}	2.98×10^{-8}	9.68×10^{-7}

Linear Relationships between log p_i and log (O/H). Consideration of Figures 1–6 for O/H ratios less than 0.5 reveals that the slopes of log p_i *vs.* log (O/H) for the oxidation products are nearly unity for CO and H_2O and nearly two for CO_2. The primary reason for these linear relationships is that the partial pressures of the oxidation products are related to species having constant chemical potentials (*e.g.*, C) or nearly constant partial pressures (H_2, CH_4), and competing reactions are unimportant. The limiting numerical values of these slopes can be derived on the basis of a simple model involving equilibrium constant expressions relating each species to oxygen (*i.e.*, O/H ratio) and an oxidizable species of relatively constant chemical potential (*e.g.*, C, CH_4, H_2).

Under the conditions outlined above, consideration of Equation 15 leads to the conclusion that log [CO] *vs.* log [O]

$$C_{(s)} + O \rightleftarrows CO \ldots\ldots\ldots K_9 \qquad (15)$$

$$[CO] = K_9[O]$$

or log [O/H] has a slope of unity. Similarly, from Equation 16:

$$C_{(s)} + 2O \rightleftarrows CO_2 \ldots\ldots\ldots K_{10} \qquad (16)$$

$$[CO_2] = K_{10}[O]^2$$

a plot of log $[CO_2]$ *vs.* log [O/H] has a slope of two. Finally, from Equation 17:

$$H_2 + O \rightleftarrows H_2O \ldots\ldots\ldots K_{11} \qquad (17)$$

$$[H_2O] = K_{11}[H_2][O]$$

and since the partial pressure of H_2 is nearly constant in the region being considered, log $[H_2O]$ *vs.* log (O/H) has a slope of unity.

In the region of O/H greater than 0.5, the decrease in the partial pressures of H_2 and H_2O can be accounted for largely on the basis of dilution effects. The more rapid disappearance of CH_4 than that of H_2 or H_2O indicates that oxidation effects in addition to dilution are contributing to its disappearance.

Minor Species. At temperatures below 1100° K., ethane is the only minor species present in excess of 10^{-6} atm, showing a maximum for a given O/H ratio in the region of 700° K. At 1300° K. ethylene is present at low O/H ratios. At 1500° K. acetylene reaches a partial pressure of 10^{-5} atm., while ethylene is increasing with temperature at a much slower rate.

Carbon Deposition Boundaries. A convenient and informative method for the presentation of the carbon deposition boundaries for the ternary CHO system is a set of triangular coordinates. The generality of this simple presentation becomes clear when it is recognized that C:H:O ratios of the system completely determine whether or not carbon will form from a given reactant composition. Thus, a single set of triangular CHO coordinates may be used to completely designate the carbon deposition regions. The effect of varying the hydrogen or oxygen content of any carbon containing system as in hydrogenation or oxidation can also be determined by use of the triangular CHO diagram.

In addition to the representation of the carbon deposition boundaries, the triangular diagram may be used to show those CHO composition regions where free oxygen, free hydrogen, and solid carbon are important as major species at equilibrium, as shown in Figure 7. In the central region bounded by the above areas, the five most important gaseous species, CO, CO_2, H_2, CH_4, and H_2, are present in varying amounts, and solid carbon may or may not be present, depending on the C:H:O ratios and the temperature, as discussed in the preceding sections. These zones are indicated in Figure 7. The central, enclosed region of the diagram is the most important, and will be discussed in detail.

Carbon deposition boundaries were computed from the detailed calculations of the gas phase compositions in equilibrium with graphite which were described above. The C:H:O atom ratios were determined directly from the gas phase compositions and are summarized in Table IV. These data are as accurate as the APIRP # 44 equilibrium data (*24*) used in the calculations.

The carbon deposition boundary for 500° K. is shown in Figure 8; above this line, solid carbon is present at equilibrium; below this line, solid carbon is absent. This boundary line represents the C:H:O atom ratios of the gas phase in equilibrium with carbon. This boundary is useful for the determination of the variation of the CHO gas phase ratios with a given change in the over-all CHO ratios of any given reactant mixture. In the presence of carbon, the gas phase composition is determined by the O/H ratio. Of particular interest is the prediction of reactant compositions which will not result in carbon deposition on achieving thermodynamic equilibrium. The lever rule may be used to calculate the exact amount of carbon which, at equilibrium, will be deposited from or consumed by a given C:H:O mixture.

In order to illustrate the utility of Figure 8, consider the oxidation process for a mixture of over-all composition *a* (see Figure 8), prepared by mixing C_nH_{2n} and H_2O. This mixture, on approaching thermodynamic equilibrium, will deposite carbon, causing the gas phase composition to move along line *aC* toward *d*, and will have a gas phase composition at equilibrium represented by *d* in Figure 8. The amount of carbon deposited can be calculated by the lever rule (7). On oxidation of mixture *a*, the overall composition of the system moves along line *aO* toward point *b*. The equilibrium gas phase composition follows line *db*, during the oxidation process. On arrival at point *b*, all solid carbon which was originally deposited will have been consumed, leaving only the gas phase of composition *b*. The composition of this gas phase will then move along line *bO* toward c during further oxidation. On arrival at point c, the system is completely oxidized and contains essentially CO_2 and H_2O.

Following a similar line of reasoning to that discussed above, the oxidation of any CH or CHO compound or mixture of compounds is represented by a straight line joining the O vertex with the point on the CHO diagram representing the over-all composition of the system. For example, the line joining C_nH_{2n} and the O vertex represents the oxidation of not only C_nH_{2n}, but also many other CHO compounds such as $(CH_2)_2O$ and HCOOH or mixtures of compounds which have an overall atom fraction represented by some point on this line. The line passing from the C vertex through the CHO composition point of interest intersects the carbon deposition boundary at a point representing the gas phase composition at equilibrium. It is interesting to note that most of the molecules indicated in Figure 8 lie above the carbon deposition boundaries for most of the temperature range considered (cf. Figure 9).

The results shown in Table IV are plotted in Figure 9. The solid lines and the 298° K. dashed line represent the conditions for which complete calculations were made. The remaining dashed lines were obtained by interpolation from high precision crossplots of the data for the solid lines. All intercepts on the C—O and C—H axes were obtained from precise thermodynamic calculations using material balance expressions together with the following equations:

C—O Axis

$$CO_2 + C \rightleftarrows 2CO \qquad (18)$$

$$K_{eq} = \frac{[CO]^2}{[C][CO_2]} = \frac{[CO]^2}{[CO_2]}$$

C—H Axis

$$CH_4 \rightleftarrows 2H_2 + C \qquad (19)$$

$$K_{eq} = \frac{[H_2]^2[C]}{[CH_4]} = \frac{[H_2]^2}{[CH_4]}$$

The intercept data are presented in Table V. The boundary for 298° K. in Figure 9 represents the situation where, mathematically, liquid water was not allowed to form and is therefore most useful for interpolation purposes.

From the detailed gas phase compositions for this system which have already been discussed, it is known that above 1100° K. the major gas phase species are H_2 and CO. Figure 9 shows that above 1100° K. the carbon deposition boundary is an essentially straight line joining the points H and CO. The relative amounts of these species may then be calculated graphically from Figure 9. Below 1100° K., the other species become increasingly important and the gas phase composition may no longer be determined by simple graphical calculations. However, the ratios of various gas phase species such as CO/CO_2 and H_2/CH_4 may be determined using the appropriate intercepts on the H—C and C—O axes. The progressive fanning of the intercepts toward CH_4 and CO_2 at the lower temperatures is due to the fact that these species are present in larger amounts at the lower temperatures. The same holds true for the lowering of the lines towards H_2O at the lower temperatures.

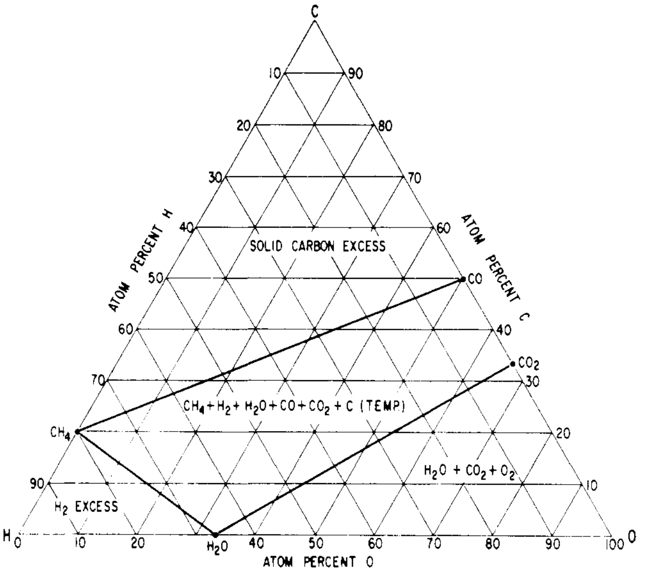

Figure 7. Regions of the CHO diagram

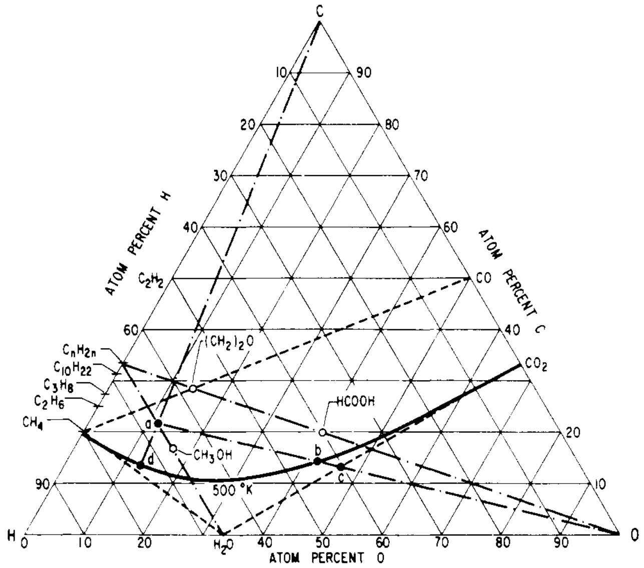

Figure 8. Carbon deposition from, and oxidation of a CHO fuel at 500° K. (Composition points for other fuels are also indicated.)

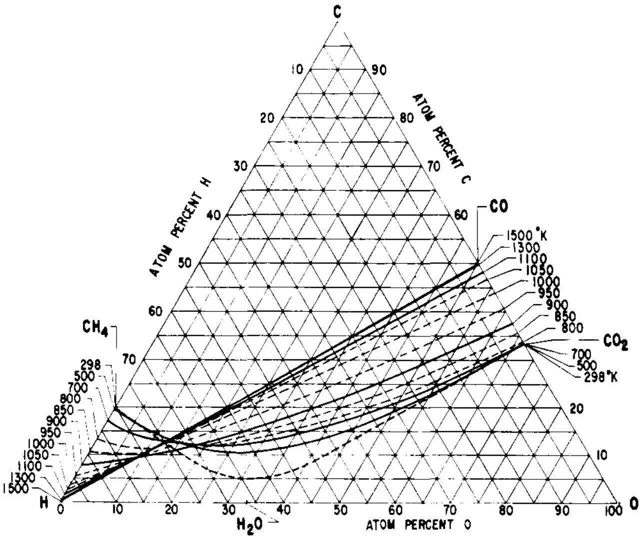

Figure 9. Carbon deposition boundaries for the CHO system at 1 atm.

Table IV. Gas Phase Atom Ratios in the CHO System at the Carbon Deposition Boundaries (1 atm. press.)

	C/O Ratio						
H/O Ratio	298° K.	500° K.	700° K.	900° K.	1100° K.	1300° K.	1500° K.
38.0000	9.00157	8.92606	7.50768	3.40036	1.52131	1.13144	1.04420
24.6667	5.669[illegible]2	5.63484	4.74679	2.28322	1.30140	1.08007	1.02737
18.0000	4.0038[illegible]	3.99490	3.37845	1.73292	1.19201	1.05451	1.01901
11.3333	2.33993	2.36804	2.03486	1.19783	1.08373	1.02926	1.01072
8.00000	1.51021	1.57026	1.38835	0.944136	1.03071	1.01694	1.00668
4.66667	0.688853	0.814109	0.793706	0.715008	0.979917	1.00518	1.00281
3.00000	0.301371	0.493658	0.548869	0.622303	0.956735	0.999884	1.00104
2.44444	0.196647	0.411581	0.484643	0.598052	0.949748	0.998312	1.00050
1.33333	0.200921	0.332040	0.406522	0.568023	0.938001	0.995754	0.999648
0.962963	0.272260	0.345027	0.404315	0.566805	0.935204	0.995196	0.999443
0.500000	0.377561	0.397594	0.428653	0.575835	0.933115	0.994861	0.999301
0.222222	0.444879	0.448932	0.462859	0.589555	0.933011	0.994954	0.999310

Table V. Carbon Deposition Boundary Intercepts on H—C and O—C Axes

	H—C Axis Intercepts		
Temp., ° K.	H/C Ratio	% H	% C
298	4.000	80.00	20.00
500	4.038	80.15	19.85
700	4.800	82.76	17.24
800	6.530	86.72	13.28
850	8.479	89.45	10.55
900	11.76	92.16	7.84
950	17.35	94.55	5.45
1000	26.17	96.32	3.68
1050	40.15	97.57	2.43
1100	60.35	98.37	1.63
1300	255.4	99.61	0.39
1500	768.2	99.87	0.13

	O—C Axis Intercepts		
Temp., ° K.	C/O Ratio	% C	% O
298	0.5000	33.33	66.67
500	0.5000	33.33	66.67
700	0.5008	33.37	66.63
800	0.5128	33.90	66.10
850	0.5552	35.70	64.30
900	0.6072	37.78	62.22
950	0.6860	40.69	59.31
1000	0.7838	43.94	56.06
1050	0.8734	46.62	53.38
1100	0.9316	48.23	51.77
1300	0.9952	49.88	50.12
1500	0.9984	49.96	50.04

CONCLUSIONS

As a result of the calculations presented here, the CHO gas phase compositions are accurately known for a wide range of O/H ratios in equilibrium with solid carbon (graphite) at one atmosphere and in the temperature range 298° to 1500° K.

The amounts of minor constituents present but not considered in the primary calculations do not affect the results to within the accuracy of the equilibrium constant data. It was found that the amount of any minor constituent can be calculated from the equilibrium data presented.

From the triangular coordinate presentation of the carbon deposition data it can be readily determined whether or not a pure compound or mixture of compounds will deposit carbon at equilibrium.

It is practical to solve directly the nonlinear equilibrium constant equations for this system. Rapidly converging solutions can be obtained on a desk calculator if desired.

ACKNOWLEDGMENT

The authors gratefully acknowledge the very able assistance of Mrs. J. Morecroft with the programming and computer calculations. Significant contributions were made by Mrs. V. Hughes and G. Holm in checking calculations and plotting data. Credit is due Miss H. Wilford for tabulating the results. The encouragement and support of H.A. Liebhafsky are appreciated.

LITERATURE CITED

(1) Boll, R.H., *J. Chem. Phys.* **34**, 1108 (1961).
(2) Boynton, F.P., *Ibid.* **32**, 1880 (1960).
(3) Brinkley, S.R., Jr., *Ibid.* **14**, 563 (1946).
(4) Brinkley, S.R., Jr., *Ibid.* **15**, 107 (1947).
(5) Brinkley, S.R., Jr., Lewis, B., *U. S. Bur. Mines, Rept.* **4805** (1952).
(6) British Gas Research Board Communications, Vol. 11-**20** (1944-48).
(7) Burton, M.S., "Applied Metallurgy for Engineers," p. 56 McGraw-Hill, New York (1956).
(8) *Chem. Eng. News* **40**, 23 (Apr. 9, 1962).
(9) *Ibid.* **40**, 64 (Apr. 16, 1962).
(10) Dorn, W.S., *J. Chem. Phys.* **32**, 1490 (1960).
(11) Duff, R.E., Bauer, S.H., *Ibid.* **36**, 1754 (1962).
(12) Greyson, M., Demeter, J.J., Schlesinger, M.D., Johnson, G.E., Jonakin, J., Myers, J.W., *U. S. Bur. Mines Rept.* **5137** (1955).
(13) Krieger, F.J., White, W.B., *J. Chem. Phys.* **16**, 358 (1948).
(14) Mayland, B.J., Hays, G.E., *Chem. Eng. Prog.* **45**, 452 (1949).
(15) Montgomery, C.W., Weinberger, E.B., Hoffman, D.S., *Ind. Eng. Chem.* **40**, 601 (1948).
(16) Muraosa, K., *Kogyo Kagaku Zasshi* **64**, 1782 (1961).
(17) *Ibid.*, 1933 (1961).
(18) *Ibid.*, 1939 (1961).
(19) Naphtali, L.M., *J. Chem. Phys.* **31**, 263 (1959).
(20) Newman, L.L., *Ind. Eng. Chem.* **40**, 559 (1948).
(21) Oliver, R.C., Stephanou, S.E., Baier, R.W., *Chem. Eng.* **69**, No. 4, 121 (1962).
(22) Potter, R.L., Vanderkulk, W., *J. Chem. Phys.* **32**, 1304 (1960).
(23) Reitmeier, R.E., Atwood, K., Bennett, H.A., Jr., Baugh, H.M., *Ind. Eng. Chem.* **40**, 620 (1948).
(24) Rossini, F.D., Pitzer, K.S., Arnett, R.L., Braun, R.M., Pimentel, G.C., American Petroleum Institute Research Project 44, Carnegie Press, Pittsburgh, Pa., 1953.
(25) White, W.B., Johnson, S.M., Dantzig, G.B., *J. Chem. Phys.* **28**, 751 (1958).

Received for review February 25, 1963. Accepted March 17, 1964. This work was supported in part by the Advanced Research Projects Agency (Order Number 247-61) through the United States Army Engineer Research and Development Laboratories, Ft. Belvoir, Va., under Contract No. DA-44-009-ENG-4853. Supplementary material to this article has been deposited as Document No. 7908 with the ADI Auxiliary Publications Project, Photoduplication Service, Library of Congress, Washington 25, D. C. A copy may be secured by citing the Document Number and by remitting $6.25 for photoprints or $2.50 for 35 mm. microfilm. Advance payment is required. Make checks or money orders payable to: Chief, Photoduplication Service, Library of Congress.